

RESEARCH ARTICLE

Effects of Human Adipose-derived Stem Cells and Platelet-Rich Plasma on Healing Response of Canine Alveolar Surgical Bone Defects

Reihaneh Shafieian, DDS, PhD; Maryam Moghaddam Matin, PhD; Amin Rahpeyma, DDS; Alireza Fazel, PhD; Hamideh Salari Sedigh, PhD; Ariane Sadr Nabavi, PhD; Halimeh Hassanzadeh, MSc; Alireza Ebrahimzadeh-Bideskan, PhD

Research performed at Mashhad University of Medical Sciences, Mashhad, Iran

Received: 25 April 2017

Accepted: 05 August 2017

Abstract

Background: Due to the known disadvantages of autologous bone grafting, tissue engineering approaches have become an attractive method for ridge augmentation in dentistry. To the best of our knowledge, this is the first study conducted to evaluate the potential therapeutic capacity of PRP-assisted hADSCs seeded on HA/TCP granules on regenerative healing response of canine alveolar surgical bone defects. This could offer a great advantage to alternative approaches of bone tissue healing-induced therapies at clinically chair-side procedures.

Methods: Cylindrical through-and-through defects were drilled in the mandibular plate of 5 mongrel dogs and filled randomly as following: I- autologous crushed mandibular bone, II- no filling material, III- HA/TCP granules in combination with PRP, and IV- PRP-enriched hADSCs seeded on HA/TCP granules. After the completion of an 8-week period of healing, radiographic, histological and histomorphometrical analysis of osteocyte number, newly-formed vessels and marrow spaces were used for evaluation and comparison of the mentioned groups. Furthermore, the buccal side of mandibular alveolar bone of every individual animal was drilled as normal control samples (n=5).

Results: Our results revealed that hADSCs subcultured on HA/TCP granules in combination with PRP significantly promoted bone tissue regeneration as compared with those defects treated only with PRP and HA/TCP granules ($P<0.05$).

Conclusion: In conclusion, our results indicated that application of PRP-assisted hADSCs could induce bone tissue regeneration in canine alveolar bone defects and thus, present a helpful alternative in bone tissue regeneration.

Keywords: Adipose tissue, Dog, Osteogenesis, Stem cells, Tissue engineering

Introduction

Loosing teeth following considerable bone loss due to severe trauma, massive infection or invasive tumors is a common problem in dentistry (1). However, replacing lost teeth in defective sites by dental implants often encounters bone insufficiency and the patient has to go under secondary surgeries for ridge augmentation by autologous bone (1). Although autologous bone grafting has been considered as the gold standard approach to fulfill the bony lesions, this procedure has some disadvantages including donor site morbidity, nerve injury, insufficient ultimate volume

especially in large-sizes defects and pathologic fractures (2). Thus, bone tissue engineering strategies has become an attractive method for ridge augmentation and great attention is paid to its different aspects for maximizing its efficiency. Bone tissue engineering strategy has three main components including stem cells for osteogenesis, growth factors for osteoinduction and biodegradable scaffolds for osteoconduction (3). Although bone marrow-derived mesenchymal stem cells (BMSCs) have been under the greatest focus in tissue engineering strategies, the invasive and painful procedure for their

Corresponding Author: Alireza Ebrahimzadeh Bideskan, Department of Anatomy and Cell Biology, School of Medicine, Mashhad University of Medical sciences, Mashhad, Iran
Email: EbrahimzadehBA@mums.ac.ir



THE ONLINE VERSION OF THIS ARTICLE
ABJS.MUMS.AC.IR

harvest has led to seek for alternative sources of stem cells (4). Adipose tissue-derived mesenchymal stem cells (ADSCs) have been considered an appropriate candidate for bone tissue reconstruction due to their high abundance in adipose tissue and easy extraction procedure (5). Recent studies have revealed that ADSCs exhibit great immunomodulatory properties due to absence of major histocompatibility complex-II (MHC-II) expression (6). In addition, it has been shown that through various soluble factors, ADSCs prevent dendritic cell differentiation, T-cell immunologic responses and eosinophilic inflammation reactions (7). Due to high accessibility of ADSCs derivable from human lipoaspirates and the inexpensive extraction procedure, human adipose tissue-derived mesenchymal stem cells (hADSCs) have become an appropriate alternative in tissue engineering applications in veterinary field (6).

Bone metabolism is considered a multifactorial array of biological processes including matrix deposition by osteoblasts as well as resorption by osteoclasts, which are exerted in a very tiny concert under the rule of various growth factors (8). Growth factors and signals needed for osteoinduction can be inserted into the microenvironment by adding platelet-rich plasma (PRP). PRP is a natural combination of various growth factors and cytokines released from activated platelets and can be prepared easily (9). Several basic growth factors secreted from de-granulated platelets include platelet-derived growth factor (PDGF), transforming growth factor (TGF), vascular endothelial growth factor (VEGF) and insulin-like growth factor-1 (IGF-1) which can then bind to their receptors on mesenchymal stem cells (MSCs), fibroblasts, osteoblasts and endothelial cells and thus, perform their effect on tissue repair and recovery (10). Although some evidence on the positive effect of PRP in bone tissue regeneration has been reported, further studies have come to conflicting results (11, 12). Thus, it seems that more investigations about the aptitude of PRP on osteogenesis is required.

An appropriate scaffold for bone tissue engineering should offer high degrees of biocompatibility and resorb ability, alongside with presentation of a suitable interface for cell attachment, proliferation and differentiation (3, 13, 14). Among different biomaterials proposed for bone tissue engineering, calcium phosphate (CaP)-based scaffolds have been widely investigated for healing of various-sized osseous defects in maxillofacial, dental and orthopedic applications due to their high similarity to bone composition and provision of an osteoconductive micro-surface (15). Although CaP-based scaffolds are known to own a high degree of calcium and phosphorous which are of essential ions for bone deposition and remodeling, they have exhibited a fast dissolution rate and thus, a low mechanical strength (3). Therefore, CaP-based scaffolds are often used in the form of biphasic hydroxy apatite/tri-calcium phosphate (HA/TCP) ceramics due to the low degradation rate and high mechanical strength of hydroxy apatite (HA) (16). Thus, HA/TCP ratio, range of porosity, pore size and specific surface topography are of important factors affecting the efficacy of the scaffold in bone tissue regenerative capacity (16).

It has been demonstrated that 30/70 HA/TCP (30% wt HA: 70% wt TCP) could lead to better biological and cellular outcomes (17). In regards of surface topography, the literature indicated that a concave surface is much more suitable for cell adhesion and differentiation in comparison to the convex ones (18). Greater surface area due to high porosity favors cell ingrowth, matrix deposition and vessel invasion which are all of principal factors affecting the osteoinductivity of the scaffold (19).

Recently, a suitable animal model selection has become one of the most important concerns in tissue engineering procedures (20). Dogs have been accepted as an appropriate animal model in orthopedic surgeries from a long time ago due to their similarities to human beings in the healing response of bone tissue (21).

To the best of our knowledge, this is the first study conducted to evaluate the potential therapeutic capacity of PRP-assisted hADSCs seeded on HA/TCP granules on regenerative healing response of canine alveolar surgical bone defects.

Materials and Methods

hADSCs isolation and identification

The use of human MSCs was approved by Ethical Committee Acts of Mashhad University of Medical Sciences. Liposuction aspirates obtained from plastic surgery of healthy volunteers were subjected to ADSCs extraction procedure, as described previously (5). Briefly, fat specimens underwent extensive washing by phosphate-buffered saline (PBS) supplemented with penicillin-streptomycin (PS), following by digestion with 0.1% collagenase type I (Invitrogen) at 37°C which was neutralized by 10% fetal bovine serum (FBS) (Gibco). After centrifugation at 800 *g* for five min, the pellet was re-suspended and seeded onto T25 flasks (Nunc). Dulbecco's modified Eagle's medium (DMEM) supplemented with 10% FBS was then added to the flasks. After 24-48 h, unattached cells were washed away and cultures were fed with fresh medium, maintaining at 37°C as well as 5% CO₂. Upon reaching 70-80% confluence, cells were trypsinized and extended on new flasks until passage 3 (P3) from which, cells were trypsinized and destined for implantation into osseous defects. To confirm of the adipose-derived stem cell nature of isolated cells, collected cells at P3 were exposed to flowcytometric analyses (BD Accuri C6 cytometer) to verify the expression of specific cell surface antigens. Our employed antibodies for FACS studies included mouse anti-CD44 polyclonal antibody, rabbit anti-CD34 polyclonal antibody (from antibodies-online, Aachen, Germany), mouse anti- CD90 monoclonal antibody (from Novus Biologicals, Littleton, Colorado, USA), and rabbit anti-CD45 polyclonal antibody (from Bioss Inc., Woburn, MA, USA) (5).

In vitro differentiation assays

Identification of isolated ADSCs was verified through *in vitro* differentiation of isolate cells at P3 toward adipogenic and osteogenic lineages (5). Maintenance of isolated cells in standard growth medium induced

mesoderm-derived phenotype of MSCs. Adipogenic differentiation was induced via maintenance in 50 mg/mL ascorbate-2-phosphate, 100 nM/L dexamethasone and 50 mg/mL indomethacin (Sigma). After a period of 21 days, fat vacuoles were stained once the cells were fixed with 10% formalin and incubated with 0.5% Oil red O (Sigma). Maintenance in osteogenic induction medium containing 50 µg/ml ascorbate-2-phosphate, 100 nM dexamethasone and 10 mM β-glycerol phosphate (Sigma) encouraged osteogenic differentiation of P3 cells. After a time of 21 days, the cells were fixed with ethanol and incubated with 0.1% Alizarin Red S (Sigma) for mineralized nodule staining. All the experiments were performed in triplicate to validate statistical analyses.

Biomaterial provision

Consumed biomaterials in this study were a kind of synthetic biomaterial composed of HA/TCP granules with the ratio of 30:70 (%weight; TCP: 70), general porosity of estimated 70±5 (%volume) and a range of 0.5-2 mm in size (OSTEON™ II, Korea).

Preparation of ADSCs/scaffold combination for implantation

One day prior to implantation, a combination of 1×10^6 hADSCs at P3 diluted in 2 mL of culture medium were firstly seeded on the HA/TCP granules in order to attach to the scaffold and then the combination was implanted into the osseous defects.

Scanning electron microscopy (SEM) analysis

SEM observation of HA/TCP granules subcultured with hADSCs was performed as a qualitative analysis (22). Briefly, after fixation of prepared scaffold/ADSCs constructs with 2.5% glutaraldehyde, and dehydration through ascending concentrations of ethanol, the specimens were sputter-coated with gold and examined under a scanning electron microscopy (Leo, Germany).

PRP preparation

Before the beginning of each surgery, 15 mL of venous blood from each animal was drawn and discharged into sterile heparinized tubes which were under constant, gentle agitation. These tubes then underwent a two-step centrifugation process in order to separate the platelets including a 10-minute centrifugation at 250 g to create three basic parts of blood suspension and a 10-minute centrifugation at 1000g for rather separating platelet-rich part. PRP was then applied to the defective sites after activation (23).

Animal Model of Surgery

All animal experiments in this study were performed in accordance with the Ethical Committee for Animal Care and Use of Mashhad University of Medical Sciences, Ethical Committee Acts (Ethical approval number: 940024). Also, all animal procedures were performed in accordance with NIH animal care guidelines.

Five adult, male mongrel dogs with the mean age of 2 years were housed in individual cages at Animal

Research Center of Mashhad Dentistry Faculty for two weeks prior to any surgery. The environment was precisely controlled for light (12 hr. light: 12 hr. dark photoperiod) and temperature (20 ± 2 °C) with free access to healthy water and commercially balanced dry food (France). Under general anesthesia, all mandibular premolars were extracted and after a one-month period of healing, two through-and-through defects perpendicular to the lateral cortex were drilled in each side of mandible with a 10 mm-diameter trephine bur. Then, surgically-created defects were filled randomly as following: I- autologous crushed mandibular bone (positive control), II- no filling material (negative control), III- HA/TCP granules in combination with PRP, and IV- hADSCs seeded on HA/TCP granules in combination with PRP. Furthermore, the buccal side of mandibular alveolar bone of every individual animal was drilled as normal control samples (n=5). These samples present the normal structure of each canine osseous tissue. Prior to surgery, pre-medication was executed via an intramuscular injection of 2 mg/kg xylazine-HCl (2% xylazine, Alfasan International BV, Woerden, Netherlands). General anesthesia was induced by an intravenous injection of 10 mg/kg ketamin-HCl (Alfasan International BV, Woerden, Netherlands) and 0.5 mg/kg diazepam (ZEPADICVR, Caspian Tamin Pharmaceutical, Iran), which was maintained under the supervision of a veterinarian (SS.H.). All the surgical procedure was performed under aseptic conditions. Also for the next 3 days, all the animals were treated by intramuscular analgesic (Tramadol, 2 mg/kg) and antibiotic (Ceftriaxone 22 mg/kg) injections and examined for any sign of intraoral infection or wound dehiscence.

Radiographic analysis

Mandibular defective sites of each animal were imaged right away after the surgery and after the completion of healing period. The images were scored using a four-point ordinal scale to evaluate both the radiographic density and radiographic height, as described previously [Table 1](24).

Histological Examination

After 8 weeks, all the animals were scarified by intravenous injection of an overdose of ketamine-HCl under general anesthesia. Then, sample retrieval from each defective site was excised by a 2 mm-diameter trephine bur while normal control samples were drilled from the buccal side of mandibular first molars. Overall, a total of 20 thorough-and-thorough mandibular defects of 5 mongrel dogs in 4 groups (n=5) were gone under sample retrieval for further assessments. Moreover, 5 more samples as the normal control group were obtained from the buccal side of mandibular alveolar bone of each individual animal (n=5). So taken as a whole, 25 samples of 5 mongrel dogs were acquired and subjected to investigation. After fixation in buffered formaldehyde and decalcification in formic acid, all the specimens were proceed according to routine histological methods, paraffin embedded and then cut into 5µm-thick sections for hematoxylin-eosin (H&E)

Table 1. Established criteria for radiological evaluation of newly-formed bone

I- radiographic density	
No evidence of bone formation	1
Density less than that of adjacent cancellous bone	2
Density greater than or equal to that of adjacent cancellous bone	3
Density greater than or equal to that of adjacent cortical bone	4
II-Radiographic height	
Up to 25% fill of height in defect area	1
Between 26%-50% fill of height in defect area	2
Between 51%-75% fill of height in defect area	3
Between 76%-100% fill of height in defect area	4
Total point possible per category	
I- radiographic density	4
II-Radiographic height	4
Possible total score	8

as well as Alizarin Red staining. Histological sections were then investigated by an optical microscope (Olympus, Japan) for any evidence of inflammation, new bone formation and existence of active osteoblasts and osteocytes (25).

Quantification of osteocytes

The number of existing osteocytes throughout the newly-formed bone tissue was counted in Alizarin Red-stained sections of each group. To accomplish this, stained samples were photographed using a light microscope (Olympus BX51, Japan) (40x objective lens) and high-resolution camera, then the images were transferred to the computer. Afterwards, cell counting continued using a special counting frame. The number of osteocytes per unit area (mm^2) (N_A) was evaluated using the following formula in which $\sum Q$ is the sum total of counted osteocytes in the sections, a/f is the surface area correlated with each frame, and $\sum P$ is the totality of frame-related points hitting the described space (26).

$$N_A = \frac{\sum Q}{a/f \cdot \sum P}$$

Histomorphometrical Analysis

The mean surface area of freshly established blood vessels as well as marrow spaces throughout the newly generated bone tissue were measured for each group. Five Alizarin Red-stained tissue sections were selected randomly for this analysis. To accomplish this, the surface area of identifiable blood vessels as well as marrow spaces were calculated and reported then as a fraction ratio of bone surface area under magnification 100x and 20x, respectively.

Statistical analysis

Statistical analysis was performed by SPSS 11.5

using ANOVA and Friedman statistical tests. *P values* lower than 0.05 were considered to be statistically significant.

Results

hADSCs characterization and expansion

Isolated cells from the aspirated adipose tissues were successfully passaged *in vitro* and displayed fibroblastic-like appearance of MSCs. In addition, multipotential capacity of the cultured cells at P3 including osteogenic and adipogenic differentiation was established through appearance of calcium deposits and lipid vacuoles, respectively [Figure 1]. Furthermore, positive expression of CD44 and CD90 antigens as well as negative expression of CD45 and CD34 markers were also evaluated by flow cytometry which strongly confirmed adipose-derived stem cell nature of isolated cells [Figure 2].

SEM evaluation

Positive loading of hADSCs subcultured on HA/TCP granules was assessed through SEM evaluation. Fibroblastic appearance of hADSCs and their extended cellular processes onto the concave surface, as evident indicators of cell-friendly being of our employed HA/TCP scaffold, were obviously identifiable [Figure 3].

Radiographic Evaluation

Radiographic images were labeled for a total achievable point for height and density based on the

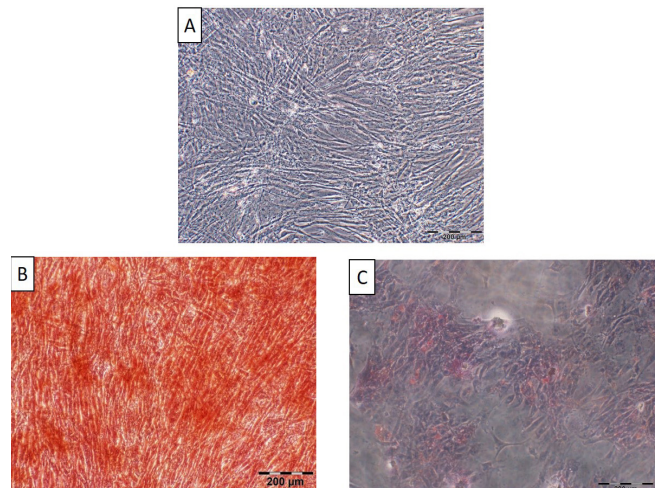


Figure 1. (A) Undifferentiated adipose-derived mesenchymal stem cells (ADMSCs) representing their fibroblastic nature, scale bar= 200 micrometer.

(B) Characterization of hADSCs by *in vitro* differentiation of the obtained cells at P3 towards the osteogenic lineage based on calcium deposits by Alizarin-Red staining 3 weeks after induction, scale bar= 200 μm .

(C) Characterization of hADSCs by *in vitro* differentiation of the obtained cells at P3 towards the adipogenic lineage through Oil red O staining 3 weeks after induction. Emerged lipid vacuoles appeared in red, scale bar= 200 μm .

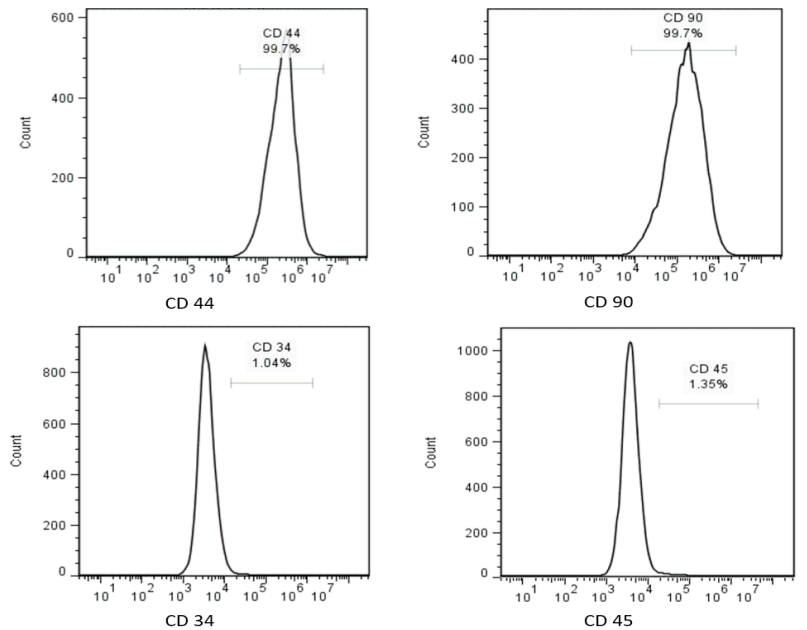


Figure 2. Phenotypic characterization of cultured ADSC at P3 revealed positive expression of CD44 and CD90 antigens as well as negative expression of CD45 and CD34 markers which strongly confirmed adipose-derived stem cell nature of isolated cells.

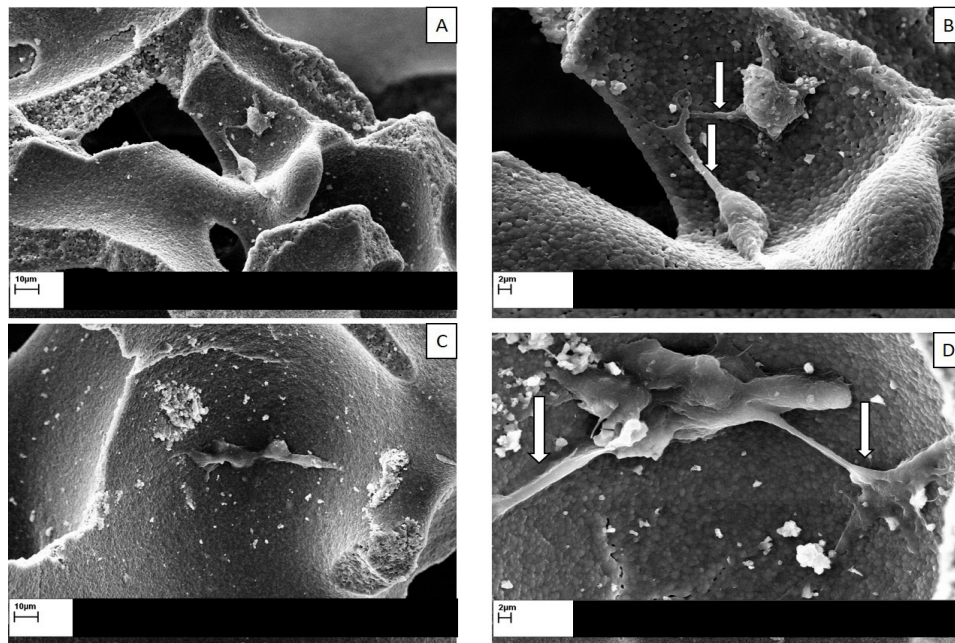


Figure 3. SEM observation of HA/TCP scaffolds sub-cultured with hADSCs, with their fibroblast-like processes extended into the scaffold after 24 h of incubation (indicated by white arrows). Panel A&C: scale bar= 10 μm (low magnification); Panel B&D: scale bar= 2 μm (high magnification).

four-point ordinal scale explained before. The mean scores of the studied groups showed significant differences [Figure 4; 5]. The mean score of the group I was significantly higher comparing to that of groups II

($P < 0.001$), III ($P < 0.01$) and IV ($P < 0.05$). In addition, the mean score of group IV was significantly higher than that of group II ($P < 0.001$) and III ($P < 0.01$). Furthermore, the mean score of group III was significantly higher

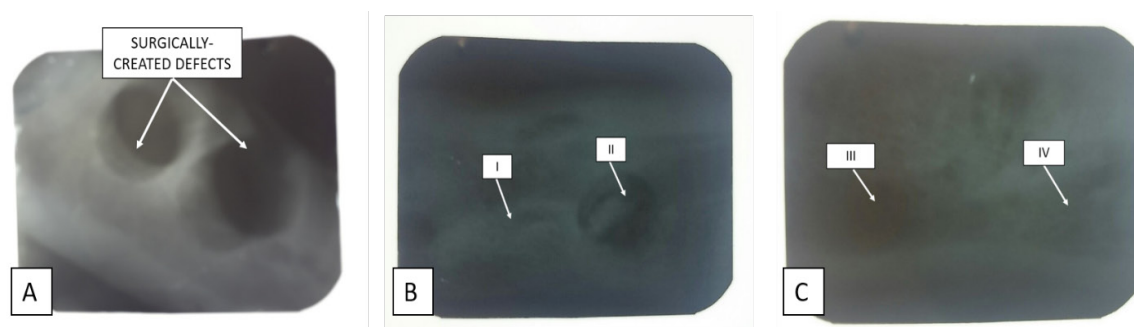


Figure 4. Radiographic images of post-operated surgical defects (A) and after the completion of an 8-week period of healing (B,C). I= defective sites + autologous bone, II= defective sites left empty, III= defective sites + PRP+ HA/TCP scaffolds, IV= defective sites + HA/TCP scaffolds + hADSCs + PRP.

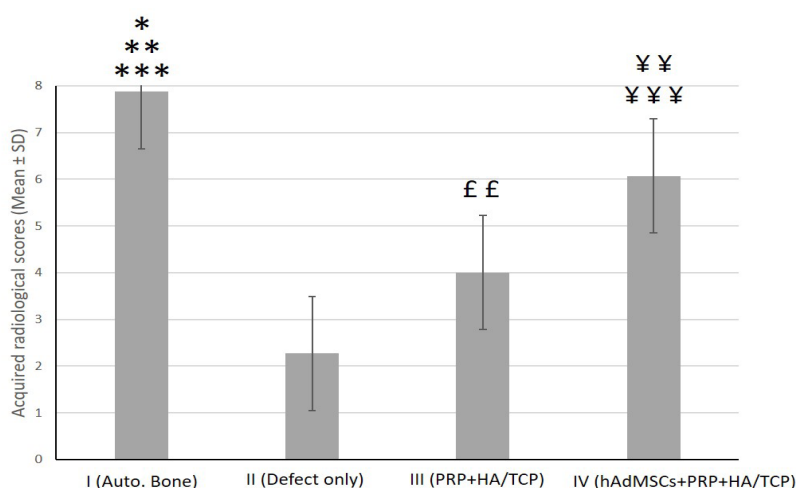


Figure 5. Quantitative assessment of the mean score acquired by radiographic images of surgically-created osseous defects after 8 weeks. The mean score of the group I was significantly higher when compared to that of groups II (** $P < 0.001$), III (** $P < 0.01$) and IV ($P < 0.05$), respectively. Score of group IV was significantly higher than that of groups II (** $P < 0.001$) and III (** $P < 0.01$). The mean score of group III was significantly higher than that of group II ($P < 0.01$).

than that of group II ($P < 0.01$) [Figure 4; 5].

Histological examination

No significant inflammatory cell infiltrate or foreign body reaction was detected in the tissue sections of treated defects. While empty defects of group II were almost filled with soft vascularized granulation tissue, specimens of group III and IV showed different amounts of hard, mineralized tissue formation which were mainly made up of woven bone. However, thin and immature bone trabeculae containing organizations of osteocytes were visible at the center of treated defects. Rows of cuboidal-shaped osteoblasts were apparently detectable lying at the periphery of forming trabeculae. Contrary to this, the defective sites of group I were nearly provided with mature bone consisting of relatively thick and well-ordered bone trabeculae which mostly resembled to the specimens taken as normal control samples. Various-

sized particles of remained scaffold were recognizable in tissue sections of groups III and IV, but no integration with the surrounding osseous tissue was apparent. Different amounts of established marrow spaces could be detected in the newly-formed bone tissue in all the experimental groups [Figure 6].

Histomorphometrical analysis of osteocyte count

In this study, Alizarin Red-stained tissue sections taken from a total of 20 alveolar defects of the 5 dogs were evaluated quantitatively [Figure 7]. The number of recognizable osteocytes per unit surface area (mm^2) of the newly-formed bone tissue was counted to explain the extent of repair more definitely. In the present study, the mean number (\pm SD) of osteocytes per unit area (mm^2) in Alizarin Red-stained sections of normal control and I -IV experimental groups were ($3.50\% \pm 0.33$), ($3.31\% \pm 0.23$), ($0.54\% \pm 0.09$),

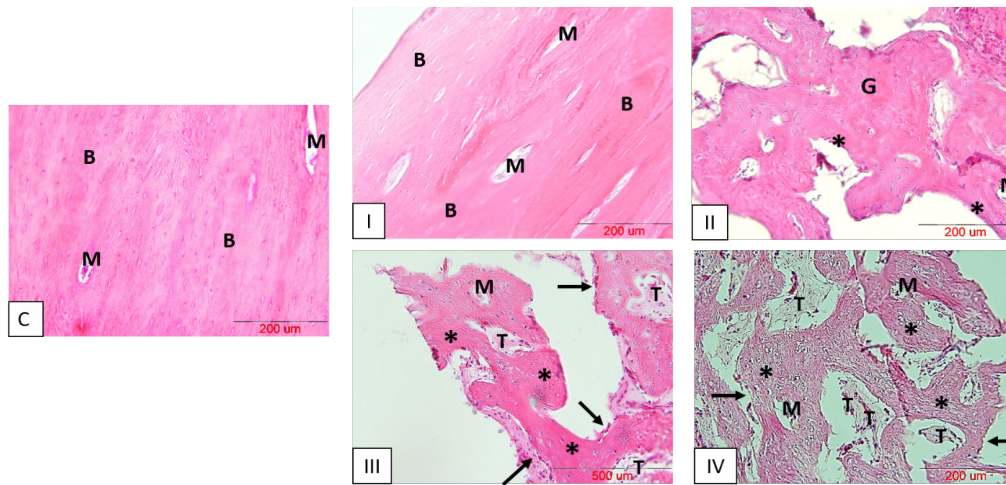


Figure 6. Histological examination of tissue repair at differently treated surgically-created osseous defects after 8 weeks (H&E staining). C= normal control sample, I= defective sites receiving particulates of autologous bone, II= defective sites left empty, III= defective sites receiving PRP+ HA/TCP scaffolds, IV- defective sites receiving HA/TCP scaffolds subcultured with hADSCs in combination with PRP; scale bars in all the photos = 200 µm. Mature bone tissue (B); Marrow spaces (M); Granulation tissue (G); Mineralized tissue (*); Remnants of scaffold (T); row of osteoblasts (black arrows).

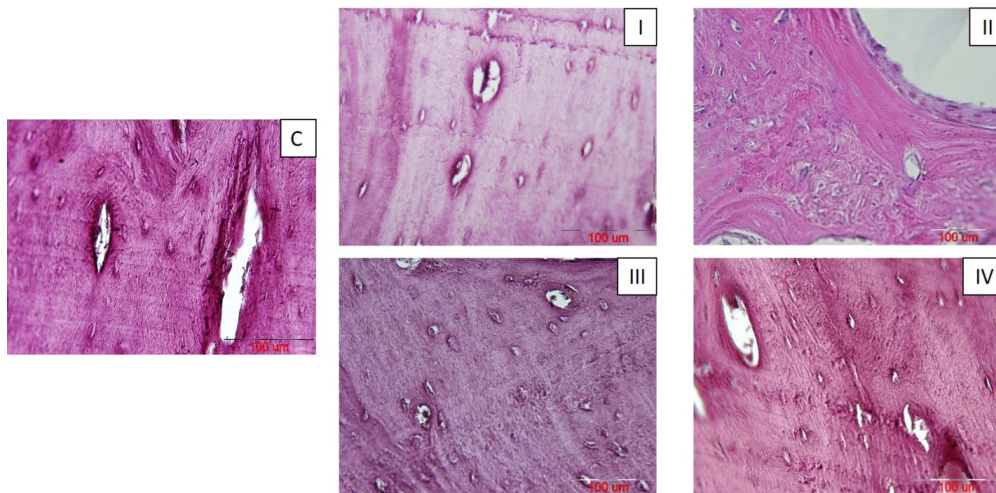


Figure 7. Alizarin Red-stained sections of bone regeneration, taken from differently treated surgically-created osseous defects after 8 weeks. C= normal control sample, I= defective sites + autologous bone, II= defective sites left empty, III= defective sites + PRP+ HA/TCP scaffolds, IV- defective sites + HA/TCP scaffolds + hADSCs + PRP, scale bars in all the photos = 100 µm.

($1.26\% \pm 0.10$) and ($2.02\% \pm 0.19$), respectively. Our statistical analysis showed that the mean number of osteocytes per unit area (N/mm^2) in the normal control group was significantly higher when compared to that of groups I ($P<0.05$), II and III ($P<0.001$) and IV ($P<0.01$). The mean number of osteocytes per unit area in group I was significantly higher comparing to that of groups II and III ($P<0.001$) and IV ($P<0.01$). The mean number of osteocytes per unit area in group IV was significantly higher than that of group II ($P<0.01$) and III ($P<0.05$). The mean number of osteocytes per unit

area in group III was significantly higher than that of group II ($P<0.05$) [Figure 8].

Histomorphometrical analysis of newly-generated blood vessels

To investigate the impact of PRP and stem cell therapy on vascularization of freshly-generating tissues, Alizarin Red-stained sections of defective sites were measured histomorphometrically for the percentage of mean surface area (\pm SD) of standing blood vessels throughout the bone tissue [Figure 9].

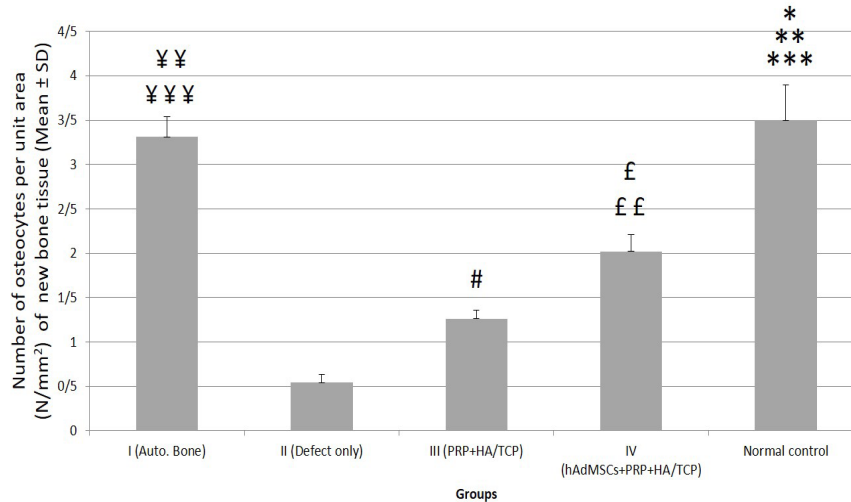


Figure 8. Quantitative assessment of the mean number (\pm SD) of detectable osteocytes per unit area (mm^2) of the bone tissue at different studied groups. Control= normal control; I= defective sites + autologous bone, II= defective sites left empty, III= defective sites + PRP+ HA/TCP scaffolds, IV= defective sites + HA/TCP scaffolds + hADSCs + PRP.

The mean number of osteocytes per unit area (N/mm^2) in the normal control group was significantly higher when compared to that of groups I ($P < 0.05$), II and III ($^{***}P < 0.001$) and IV ($^{**}P < 0.01$). The mean number of osteocytes per unit area in group I was significantly higher comparing to that of groups II and III ($^{***}P < 0.001$) and IV ($^{**}P < 0.01$). The mean number of osteocytes per unit area in group IV was significantly higher than that of group II ($^{**}P < 0.01$) and III ($^{\#}P < 0.05$). The mean number of osteocytes per unit area in group III was significantly higher than that of group II ($^{\#}P < 0.05$).

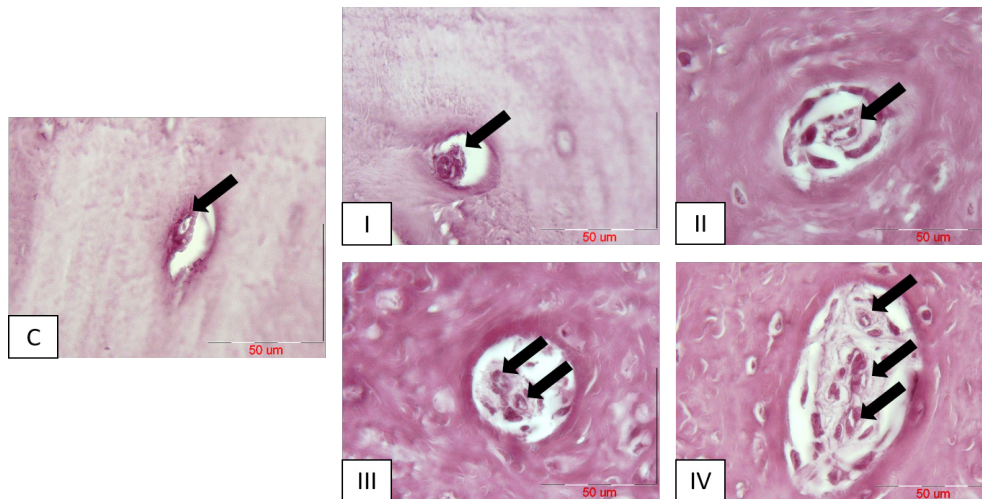


Figure 9. Vessel formation (black arrows) in Alizarin Red-stained sections of different groups, C= normal control sample; I= defective sites + autologous bone, II= defective sites left empty, III= defective sites + PRP+ HA/TCP scaffold, IV= defective sites +HA/TCP scaffold + hADSCs + PRP. Scale bar in all photos= 50 μm .

The related values were ($0.20\% \pm 0.03$), ($0.12\% \pm 0.03$), ($0.98\% \pm 0.10$), ($1.91\% \pm 0.09$) and ($0.19\% \pm 0.06$) in I, II, III, IV and normal control groups, respectively [Figure 10]. According to statistical analysis, group IV displayed the utmost percentage of the mean surface area of blood vessels and therefore, exhibited statistically increase when compared to groups I, II, normal control ($P < 0.001$) and III ($P < 0.01$). In addition,

group III demonstrated statistically significant increase in comparison to groups I, II and normal control ($P < 0.01$). The percentage of mean surface area of the blood vessels showed no significant difference among groups I, II and normal control [Figure 10]. Despite the fact that group III failed to be significantly different when compared to group I, it appeared to have a tendency toward that ($P = 0.08$).

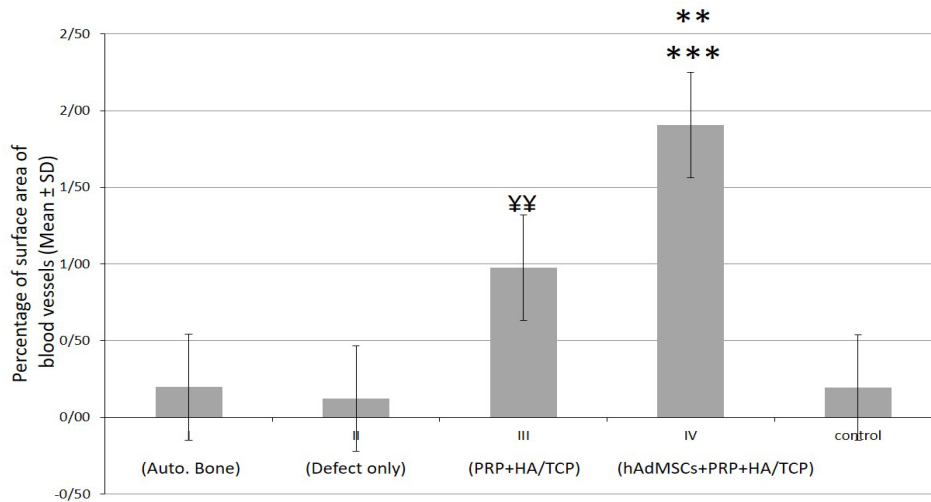


Figure 10. Quantitative assessment of the mean surface area (\pm SD) of blood vessels throughout the new bone tissue at different groups. C= normal control; I= defective sites + autologous bone, II= defective sites left empty, III= defective sites + PRP + HA/TCP scaffolds, IV= defective sites + HA/TCP scaffolds + hADSCs + PRP

The percentage of mean surface area of blood vessels in group IV showed statistically significant increase when compared to groups I, II, normal control (** $P < 0.001$) and III (** $P < 0.01$). In addition, group III demonstrated statistically significant increase in comparison to groups I, II and normal control (** $P < 0.01$). The percentage of mean surface area of the blood vessels showed no significant difference among groups I, II and normal control.

Histomorphometrical analysis of marrow spaces of the newly generated bone tissue

Alizarin Red-stained sections of defective sites were also evaluated histomorphometrically for the percentage of mean surface area (\pm SD) of established marrow spaces throughout the newly generated bone tissue [Figure 11]. The related values were (29.92% \pm 3.40), (11.80% \pm 1.71), (40.91% \pm 3.73), (54.74% \pm 4.87) and (28.94% \pm 2.50) in I, II, III, IV and normal control groups, respectively [Figure 12]. Our statistical analysis showed that the percentage of

mean surface area of established marrow spaces in group IV was significantly higher when compared to that of groups I and normal control ($P < 0.01$), II ($P < 0.001$) and III ($P < 0.05$). The related value in group III was significantly higher comparing to that of groups I and normal control ($P < 0.05$) and II ($P < 0.01$). Groups I and normal control demonstrated statistically significant increase in comparison to group II ($P < 0.01$). The percentage of mean surface area of established marrow spaces showed no significant difference between groups I and normal control [Figure 12].

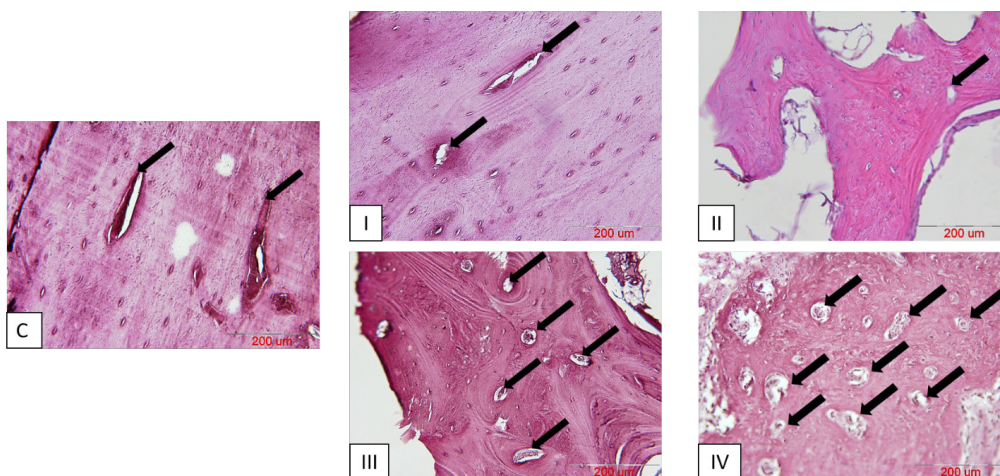


Figure 11. Established marrow spaces (black arrows) throughout the new bone tissue in Alizarin Red-stained sections of different groups, C= normal control sample; I= defective sites + autologous bone, II= defective sites left empty, III= defective sites + PRP+ HA/TCP scaffold, IV= defective sites +HA/TCP scaffold + hADSCs + PRP. Scale bar in all photos= 200 μ m.

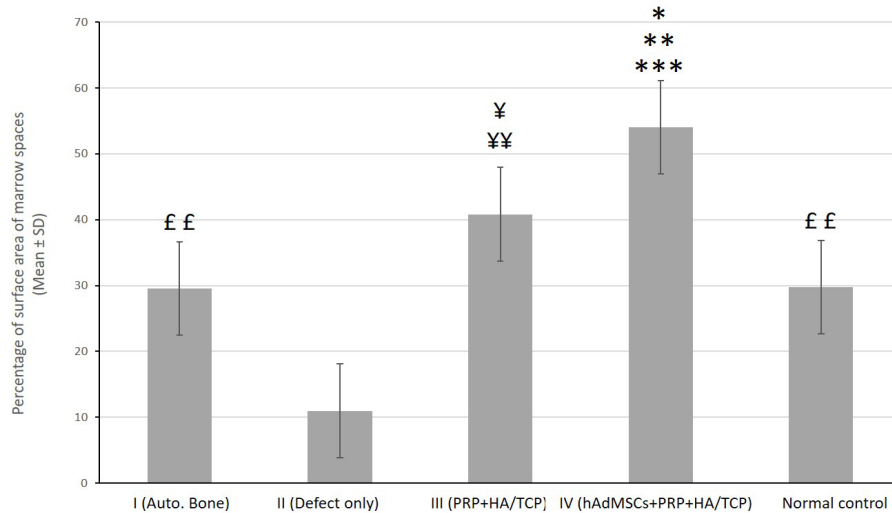


Figure 12. Quantitative assessment of the percentage of mean surface area (\pm SD) of established marrow spaces throughout the new bone tissue at different groups. C= normal control; I= defective sites + autologous bone, II= defective sites left empty, III= defective sites + PRP + HA/TCP scaffolds, IV= defective sites + HA/TCP scaffolds + hADSCs + PRP

According to statistical analysis, the percentage of mean surface area of established marrow spaces in group IV was significantly higher when compared to that of groups I and normal control (** $P < 0.01$), II (***) $P < 0.001$) and III ($P < 0.05$). The related value in group III was significantly higher comparing to that of groups I and normal control (* $P < 0.05$) and II (** $P < 0.01$). Groups I and normal control demonstrated statistically significant increase in comparison to group II (££ $P < 0.01$). The percentage of mean surface area of established marrow spaces showed no significant difference between groups I and normal control.

Discussion

This study aimed to evaluate the PRP-assisted potential efficiency of hADSCs seeded on HA/TCP scaffold on regenerative healing response of canine alveolar surgical bone defects. Our employed histomorphometrical analysis of osteocyte count, formation of blood vessels as well as marrow spaces throughout the freshly-generated bone tissue, as strong indicators of therapeutic efficiency of different treatments, revealed that PRP-enriched hADSCs subcultured on HA/TCP granules significantly promoted bone tissue regeneration when compared with those defects which were left empty or treated only with PRP and HA/TCP granules. Minimal bone tissue regeneration occurred at those osseous defects which were left empty and received no treatment. Indeed, treating the bony lesions with PRP and HA/TCP granules induced significantly greater tissue regeneration when compared to empty defects. Supplementation with hADSCs led to significantly superior repairing response of bone tissue which indicated the potential efficacy of stem cell application in treating osseous defects. Although treating the defects with autologous bone grafting led to the highest number of osteocytes among experimental groups, it presented significantly inferior outcomes in regards of vessel formation as well as marrow space establishment. Nonetheless, considering the disadvantages of autologous bone grafting especially in treating large-sized defects, stem cell application seems to present a helpful alternative in bone tissue regeneration and healing.

ADSCs have been introduced as a reliable therapeutic tool for bone tissue regenerative procedures (27). It has been demonstrated that ADSCs in combination with synthetic

scaffolds such as HA/TCP granules could induce bone tissue regeneration even in large and critical-sized defects (27).

Growth factors are considered as osteoinductive agents that facilitate signal transduction between cells and scaffolds and thus, have the potential to affect the regenerative capacity of bone tissue (28). Various growth factors, especially bone morphogenic proteins (BMPs), have been introduced and investigated as efficient osteoinductive agents in bone tissue engineering process (28). However, it has a short half-life time and its purification and usage is much expensive. Thus, development of this approach as a practical method to clinical operations seems almost impossible in near future.

PRP is regarded as a helpful therapeutic mixture of imperative growth factors naturally contained in platelets' granules which upon activation, are released and establish a series of crucial regenerative procedures throughout different tissues (10). The growth factors contained in PRP, including PDGF, TGF, VEGF and IGF-1, can stimulate a variety of receptor cells that are engaged in tissue repair and recovery such as matrix production, cellular proliferation and angiogenesis (29). Despite the considerable evidence on potential therapeutic effects of PRP on wound healing, the published data is almost confusing and contradictory. Although some studies have found no identifiable beneficial effect of PRP on tissue redevelopment, others have concluded a significant impact of PRP application on tissue regeneration (30). In our study, we found a positive effect of PRP usage on number of osteocytes, formation of blood vessels as well as marrow spaces, which are of strong indicators of bone tissue repair and regeneration.

If truth be told, therapeutic impression of PRP administration has mainly been contributed to the latent potential of its contained growth factors on recruitment of endothelial progenitor cells and promotion of angiogenesis, regarded as a crucial preliminary step to tissue repair and regeneration (31). Thus, PRP application reinforces the idea of therapeutic consequence of angiogenesis in tissue engineering approaches (10). Accordingly, we hypothesized that application of stem cells and PRP would enhance vasculogenesis in the newly-engineered bone tissue. According to the findings of this study, PRP administration significantly induced vessel formation in comparison to empty or autologous bone-received defective sites. However, the significantly highest amount of vessel formation occurred at those defects that received stem cells and PRP Simultaneously. This could occur due to the synergistic effects of various biologically active growth factors released from microvesicles of stem cells and de-granuled platelets concurrently.

Biphasic CaP-based scaffolds (BCP) including a more stable phase (HA) and a more soluble phase (TCP) have been introduced as a promising reconstructive scaffold in bone tissue regenerative procedures (17). However, this capacity is influenced by several important factors including HA/TCP ratio, range of porosity and specific surface topography (16). In this study, we selected a kind of BCP with 30/70 HA/TCP ratio (30% wt HA: 70% wt TCP), concave surface topography and high porosity of estimated 70 ± 5 (%volume). The results of this study showed that this scaffold in combination with PRP led to considerable bone tissue healing and regeneration.

It has been shown that histological structure of bone considerably differs among various species (20). In addition to bone structure, inflammatory and regenerative procedures in large mammals are more similar to human beings than smaller ones (32). Dogs are the first choice of regulatory agencies like FDA in evaluation of the efficacy and safety of an applicable method to human beings (21). However, one of the inadequacies of this research was our limited groups for study of bone healing response in the presence of various sets of bioactive materials. In addition, scarification of animals at different times could lead to obtain more valuable data on regenerative healing capacity of bone tissue under the rule of applied biomaterials.

To the best of our knowledge, this is the first study conducted to investigate the potential therapeutic capacity of PRP-assisted hADSCs seeded on HA/TCP granules on regenerative healing response of alveolar surgical bone defects in Mongrel dog. Taken as a whole, our employed functional assays revealed that application of PRP-assisted hADSCs would greatly enhance the healing process of bone tissue indicated by the number of osteocytes, amount of generated blood vessels and marrow spaces, which are of essential elements to the regenerative processes. This could offer a great advantage to alternative approaches of bone tissue healing-induced therapies at clinically chair-side procedures.

In conclusion, our results indicated that application of PRP-assisted hADSCs in combination with HA/TCP granules can induce bone tissue regeneration in large-sized canine alveolar defects and thus, present a helpful alternative in bone tissue regeneration.

There is no conflict of interest to declare.

The authors report no conflict of interest concerning the materials or methods used in this study or the findings specified in this paper.

Acknowledgements

The authors thank the Vice Chancellor for Research of Mashhad University of Medical Sciences for financial supports (Protocol Code: 940024). This article is the outcome of PhD student thesis at Anatomy and Cell Biology department. In addition, the authors gratefully appreciate the cooperation of Dr. Nasser Sanjar- Moosavi in supplying liposuction material and also Dr. Hamed Abachizadeh for his expert technical assistance. Moreover, the authors thank Fatemeh Motejaded and Abdollah Javan-Rashid for their great help.

Reihaneh Shafieian DDS PhD
Department of Anatomy and Cell Biology, School of Medicine,
Mashhad University of Medical Sciences, Mashhad, Iran

Maryam Moghaddam Matin PhD
Department of Biology, Faculty of Sciences, Ferdowsi
University of Mashhad, Mashhad, Iran
Stem Cells and Regenerative Medicine Research Group,
Academic Center for Education, Culture, and Research
(ACECR), Khorasan Razavi Branch, Mashhad, Iran
Novel Diagnostics and Therapeutics Research Group,
Institute of Biotechnology, Ferdowsi University of
Mashhad, Mashhad, Iran

Amin Rahpeyma DDS
Oral and Maxillofacial Diseases Research Center, School
of Dentistry, Mashhad University of Medical Sciences,
Mashhad, Iran

Alireza Fazel PhD
Alireza Ebrahimzadeh-Bideskan PhD
Department of Anatomy and Cell Biology, School of Medicine,
Mashhad University of Medical Sciences, Mashhad, Iran
Microanatomy Research Center, School of Medicine,
Mashhad University of Medical Sciences, Mashhad, Iran

Hamideh Salari Sedigh PhD
Department of Clinical Sciences, Faculty of Veterinary
Medicine, Ferdowsi University of Mashhad, Mashhad, Iran

Ariane Sadr Nabavi PhD
Department of Genetics, School of Medicine, Mashhad
University of Medical Sciences, Mashhad, Iran

Halimeh Hassanzadeh MSc
Department of Biology, Faculty of Sciences, Ferdowsi
University of Mashhad, Mashhad, Iran
Stem Cells and Regenerative Medicine Research Group,
Academic Center for Education, Culture, and Research
(ACECR), Khorasan Razavi Branch, Mashhad, Iran

References

1. Esposito M, Grusovin MG, Felice P, Karatzopoulos G, Worthington HV, Coulthard P. Interventions for replacing missing teeth: horizontal and vertical bone augmentation techniques for dental implant treatment. *Cochrane Database Syst Rev.* 2009; 7(4):D003607.
2. Erbe EM, Marx GJ, Clineff TD, Bellincampi LD. Potential of an ultraporous β -tricalcium phosphate synthetic cancellous bone void filler and bone marrow aspirate composite graft. *Eur Spine J.* 2001; 10(Suppl 2):S141-6.
3. Sulaiman SB, Keong TK, Cheng CH, Saim AB, Idrus RB. Tricalcium phosphate/hydroxyapatite (TCP-HA) bone scaffold as potential candidate for the formation of tissue engineered bone. *Indian J Med Res.* 2013; 137(6):1093-101.
4. Malgieri A, Kantzari E, Patrizi MP, Gambardella S. Bone marrow and umbilical cord blood human mesenchymal stem cells: state of the art. *Int J Clin Exp Med.* 2010; 3(4):248-69.
5. Naderi-Meshkin H, Matin MM, Heirani-Tabasi A, Mirahmadi M, Irfan-Maqsood M, Edalatmanesh MA, et al. Injectable hydrogel delivery plus preconditioning of mesenchymal stem cells: exploitation of SDF-1/CXCR4 axis toward enhancing the efficacy of stem cells' homing. *Cell Biol Int.* 2016; 40(7):730-41.
6. Lin CS, Lin G, Lue TF. Allogeneic and xenogeneic transplantation of adipose-derived stem cells in immunocompetent recipients without immunosuppressants. *Stem Cell Dev.* 2012; 21(15):2770-8.
7. Puissant B, Barreau C, Bourin P, Clavel C, Corre J, Bousquet C, et al. Immunomodulatory effect of human adipose tissue-derived adult stem cells: comparison with bone marrow mesenchymal stem cells. *Br J Haematol.* 2005; 129(1):118-29.
8. Tahami M, Haddad B, Abtahian A, Hashemi A, Aminian A, Konan S. Potential role of local estrogen in enhancement of fracture healing: preclinical study in rabbits. *Arch Bone Jt Surg.* 2016; 4(4):323-9.
9. Kim ES, Kim JJ, Park EJ. Angiogenic factor-enriched platelet-rich plasma enhances in vivo bone formation around alloplastic graft material. *J Adv Prosthodontol.* 2010; 2(1):7-13.
10. Dhurat R, Sukesh M. Principles and methods of preparation of platelet-rich plasma: a review and author's perspective. *J Cutan Aesthet Surg.* 2014; 7(4):189-97.
11. Butterfield KJ, Bennett J, Gronowicz G, Adams D. Effect of platelet-rich plasma with autogenous bone graft for maxillary sinus augmentation in a rabbit model. *J Oral Maxillofac Surg.* 2005; 63(3):370-6.
12. Roldán JC, Jepsen S, Miller J, Freitag S, Rueger DC, Açil Y, et al. Bone formation in the presence of platelet-rich plasma vs. bone morphogenetic protein-7. *Bone.* 2004; 34(1):80-90.
13. Ghavimi SA, Ebrahimzadeh MH, Shokrgozar MA, Solati-Hashjin M, Osman NA. Effect of starch content on the biodegradation of polycaprolactone/starch composite for fabricating in situ pore-forming scaffolds. *Polymer Test.* 2015; 43(2):94-102.
14. Ali Akbari Ghavimi S, Ebrahimzadeh MH, Solati-Hashjin M, Abu Osman NA. Polycaprolactone/starch composite: fabrication, structure, properties, and applications. *J Biomed Mater Res A.* 2015; 103(7):2482-98.
15. Gamblin AL, Brennan MA, Renaud A, Yagita H, Lézot F, Heymann D, et al. Bone tissue formation with human mesenchymal stem cells and biphasic calcium phosphate ceramics: the local implication of osteoclasts and macrophages. *Biomaterials.* 2014; 35(36):9660-7.
16. Houmard M, Fu Q, Genet M, Saiz E, Tomsia AP. On the structural, mechanical, and biodegradation properties of HA/ β -TCP robocast scaffolds. *J Biomed Mater Res B Appl Biomater.* 2013; 101(7):1233-42.
17. Hahn BD, Park DS, Choi JJ, Ryu J, Yoon WH, Lee BK, et al. Effect of the HA/ β -TCP ratio on the biological performance of calcium phosphate ceramic coatings fabricated by a room-temperature powder spray in vacuum. *J Am Ceram Soc.* 2009; 92(4):793-9.
18. Ripamonti U, Crooks J, Kirkbride A. Sintered porous hydroxyapatites with intrinsic osteoinductive activity: geometric induction of bone formation. *South Afr J Sci.* 1999; 95(8):335-43.
19. Lobo SE, Livingston Arinzech T. Biphasic calcium phosphate ceramics for bone regeneration and tissue engineering applications. *Materials.* 2010; 3(2):815-26.
20. Hörner K, Loeffler K, Holtzmann M. Comparison of the histologic structure of the compact bone of the long hollow bones of mouse, hamster, rat, guinea pig, rabbit, cat, and dog during development. *Anat Histol Embryol.* 1997; 26(4):289-95.
21. Pearce SG. Animal models for bone repair. *Eur Cell Mater.* 2007; 14(1):42-9.
22. Kang Y, Kim S, Khademhosseini A, Yang Y. Creation of bony microenvironment with CaP and cell-derived ECM to enhance human bone-marrow MSC behavior and delivery of BMP-2. *Biomaterials.* 2011; 32(26):6119-30.
23. Xie X, Wang Y, Zhao C, Guo S, Liu S, Jia W, et al. Comparative evaluation of MSCs from bone marrow and adipose tissue seeded in PRP-derived scaffold for cartilage regeneration. *Biomaterials.* 2012; 33(29):7008-18.
24. Miloro M, Haralson DJ, Desa V. Bone healing in a rabbit mandibular defect using platelet-rich plasma. *J Oral Maxillofac Surg.* 2010; 68(6):1225-30.
25. Jafarian M, Eslaminejad MB, Khojasteh A, Mashhadi Abbas F, Dehghan MM, Hassanizadeh R, et al. Marrow-derived mesenchymal stem cells-directed bone regeneration in the dog mandible: a comparison between biphasic calcium phosphate and natural bone mineral. *Oral Surg Oral Med Oral Pathol Oral Radiol Endod.* 2008; 105(5):e14-24.

26. Mohammadipour A, Fazel A, Haghiri H, Motejaded F, Rafatpanah H, Zabihi H, et al. Maternal exposure to titanium dioxide nanoparticles during pregnancy; impaired memory and decreased hippocampal cell proliferation in rat offspring. *Environ Toxicol Pharmacol.* 2014; 37(2):617-25.
27. Levi B, James AW, Nelson ER, Vistnes D, Wu B, Lee M, et al. Human adipose derived stromal cells heal critical size mouse calvarial defects. *PloS One.* 2010; 5(6):e111177.
28. Tollemar V, Collier ZJ, Mohammed MK, Lee MJ, Ameer GA, Reid RR. Stem cells, growth factors and scaffolds in craniofacial regenerative medicine. *Genes Dis.* 2016; 3(1):56-71.
29. van Bergen CJ, Kerkhoffs GM, Özdemir M, Korstjens CM, Everts V, van Ruijven LJ, et al. Demineralized bone matrix and platelet-rich plasma do not improve healing of osteochondral defects of the talus: an experimental goat study. *Osteoarth Cartilage.* 2013; 21(11):1746-54.
30. Wolf BR. An injection of platelet-rich plasma was not more effective than placebo for rotator cuff tendinopathy. *J Bone Jt Surg.* 2014; 96(10):871-8.
31. Chen FM, Wu LA, Zhang M, Zhang R, Sun HH. Homing of endogenous stem/progenitor cells for in situ tissue regeneration: promises, strategies, and translational perspectives. *Biomaterials.* 2011; 32(12):3189-209.
32. Kovacevic M, Tamarut T, Zoricic S, Bešlic S. A method for histological, enzyme histochemical and immunohistochemical analysis of periapical diseases on undecalcified bone with teeth. *Acta Stomatol Croat.* 2003; 37(3):261-73.